An *N*-Ethyl-*N*-Nitrosourea Mutagenesis Screen for Epigenetic Mutations in the Mouse

Ivona Percec,*,† Joanne L. Thorvaldsen,* Robert M. Plenge,†,[1] Christopher J. Krapp,* Joseph H. Nadeau,† Huntington F. Willard†,‡,[2] and Marisa S. Bartolomei*,[3]

**Howard Hughes Medical Institute and Department of Cell and Developmental Biology, University of Pennsylvania School of Medicine, Philadelphia, Pennsylvania 19104, †Department of Genetics, Case Western Reserve University School of Medicine, Cleveland, Ohio 44106 and ‡Center for Human Genetics, University Hospitals of Cleveland, Cleveland, Ohio 44106*

Manuscript received January 27, 2003
Accepted for publication April 4, 2003

ABSTRACT

The mammalian epigenetic phenomena of X inactivation and genomic imprinting are incompletely understood. X inactivation equalizes X-linked expression between males and females by silencing genes on one X chromosome during female embryogenesis. Genomic imprinting functionally distinguishes the parental genomes, resulting in parent-specific monoallelic expression of particular genes. *N*-ethyl-*N*-nitrosourea (ENU) mutagenesis was used in the mouse to screen for mutations in novel factors involved in X inactivation. Previously, we reported mutant pedigrees identified through this screen that segregate aberrant X-inactivation phenotypes and we mapped the mutation in one pedigree to chromosome 15. We now have mapped two additional mutations to the distal chromosome 5 and the proximal chromosome 10 in a second pedigree and show that each of the mutations is sufficient to induce the mutant phenotype. We further show that the roles of these factors are specific to embryonic X inactivation as neither genomic imprinting of multiple genes nor imprinted X inactivation is perturbed. Finally, we used mice bearing selected X-linked alleles that regulate X chromosome choice to demonstrate that the phenotypes of all three mutations are consistent with models in which the mutations have affected molecules involved specifically in the choice or the initiation of X inactivation.

EPIGENETIC gene regulation mechanisms result in chromatin modification and genome reprogramming during mammalian development. The two best-studied examples of epigenetic regulation, X inactivation and genomic imprinting, are thought to be evolutionarily related (Pannuti and Luchessi 2000). X inactivation results in the chromosome-wide silencing of one of the two X chromosomes in each cell of a female mammal (Avner and Heard 2001). Genomic imprinting results in the differential expression of the paternal and maternal alleles of specific genes (Ferguson-Smith and Surani 2001). Although both processes produce monoallelic expression of a subset of genes in the genome, imprinted genes reside in clusters throughout the autosomes and are regulated in a parent-of-origin-specific manner, while the effect of X inactivation is limited to genes on one X chromosome and the choice of which X is to be inactivated in any given embryonic cell is random. The relationship between the pathways of X inactivation and genomic imprinting is best exemplified by the extraembryonic tissues of certain rodents, including mice. In these tissues, X inactivation is imprinted with preferential silencing of the paternal X chromosome (Takagi and Sasaki 1975). Classic genetic analyses have revealed multiple molecules involved in these epigenetic pathways and have suggested that the interplay of such factors via large protein complexes is likely to be crucial to all epigenetic gene regulation mechanisms (Marin *et al.* 2000; Pannuti and Luchessi 2000). Nevertheless, details of the underlying molecular mechanisms, including which aspects are shared by or are unique to the imprinting or X-inactivation pathways, remain poorly understood. Further characterization of the components of these regulatory complexes is necessary for understanding mammalian epigenetic reprogramming.

X chromosome inactivation equalizes X-linked expression between males and females through the transcriptional silencing of a majority of genes on one X chromosome during early female development (Lyon 1961). To achieve stable silencing of one X chromosome, a cell must complete distinct stages of the pathway: selection or choice of one of the two X chromosomes, initiation and propagation of silencing, and maintenance of the inactive state during subsequent cell divisions (Avner and Heard 2001; Boumil and Lee 2001). The establishment of inactivation is under the

[1]*Present address:* Whitehead Institute Center for Genome Research, MIT, Cambridge, MA 02139.

[2]*Present address:* Institute for Genome Sciences and Policy, Duke University, Durham, NC 27710.

[3]*Corresponding author:* Department of Cell and Developmental Biology, University of Pennsylvania School of Medicine, 360 CRB, 415 Curie Blvd., Philadelphia, PA 19104.
E-mail: bartolom@mail.med.upenn.edu

control of elements within the genetically defined X-inactivation center (*Xic*) on the X chromosome. The inactive X maintains its silent state by acquiring distinct epigenetic modifications, including histone 3 lysine methylation, replication timing variation, CpG methylation, histone hypoacetylation, and enrichment with the histone variant macroH2A (Costanzi and Pehrson 1998; Chadwick and Willard 2001; Csankovszki *et al.* 2001; Heard *et al.* 2002).

At least three elements within the *Xic* are involved in the establishment of X chromosome silencing. A key component is the *Xist* gene that is required *in cis* during the early stages of inactivation for both initiation and propagation of X chromosome silencing and that represents the major silencing element early in the pathway (Brockdorff *et al.* 1991; Brown *et al.* 1991; Penny *et al.* 1996). *Tsix*, a gene antisense to *Xist*, suppresses *Xist*'s silencing activity prior to inactivation, locks in the states of the active and inactive X chromosomes, and plays an important role in imprinted X inactivation in extraembryonic tissues (Lee *et al.* 1999; Lee and Lu 1999; Mise *et al.* 1999; Lee 2000; Wutz and Jaenisch 2000; Boumil and Lee 2001). The X-controlling element (*Xce*) within the *Xic* regulates X chromosome choice in the mouse via different alleles (Cattanach and Isaacson 1965). The four *Xce* alleles that have been described, Xce^a, Xce^b, Xce^c, and Xce^d, function *in cis* to affect the probability that an X chromosome remains active (Cattanach *et al.* 1969; West and Chapman 1978; Cattanach and Papworth 1981; Johnston and Cattanach 1981; Cattanach and Rasberry 1991, 1994). The *Xce* effect results in nonrandom X-inactivation choice in *Xce* heterozygous females, but random inactivation in *Xce* homozygous females (Plenge *et al.* 2000). Mutation studies have suggested that *trans*-acting autosomal factors interact with *cis*-acting elements within the *Xic* to determine X chromosome choice (Lyon 1971; Brown and Chandra 1973; Russell and Cacheiro 1978; Rastan 1983). Recently, one *trans*-acting factor, the chromatin insulator and transcription regulator CTCF (CCC TC-binding factor), has been suggested to bind sites within the *Xic* to direct X chromosome choice (Chao *et al.* 2002). It is likely that additional *trans*-acting molecules are involved in the pathway (Percec and Bartolomei 2002).

While X chromosome inactivation specifically affects genes on the X chromosome, genomic imprinting modifies the activity of a subset of autosomal genes in a parent-of-origin-specific manner (Ferguson-Smith and Surani 2001). Imprinted genes, clustered throughout the genome in "imprinted domains," are subject to coordinate regulation. Multiple factors regulate genomic imprinting by invoking allele-specific differences in DNA methylation, chromatin structure, and gene expression similar to those documented for genes undergoing X inactivation. These modifications enable the organism to erase, set, and maintain the appropriate epigenetic state of a given allele. While some of the molecules that govern these modifications have been identified, many, including those possibly common to X inactivation and genomic imprinting, remain unknown (Bourc'his *et al.* 2001; Howell *et al.* 2001; Reik *et al.* 2001).

N-ethyl-*N*-nitrosourea (ENU) mutagenesis has been applied effectively to identify novel developmental and behavioral factors in the mouse (Habre de Angelis *et al.* 2000; Nadeau 2000; Nolan *et al.* 2000). We describe here how ENU mutagenesis screens may be applied successfully to dissect quantitative trait phenotypes of epigenetic pathways. We argue that the use of a sensitive, specific, high-throughput, and noninvasive assay with genetically matched phenotyping controls is crucial to identifying mutations with subtle effects on complex mechanisms. We previously described autosomal mutations with dominant effects on X chromosome inactivation in two pedigrees identified through a genome-wide, phenotype-driven mouse ENU mutagenesis screen for mutations with primary effects on X inactivation and mapped the mutation segregating in one pedigree to mouse chromosome 15 (Percec *et al.* 2002). We now have mapped two additional mutations on mouse chromosomes 5 and 10 in the second pedigree, fulfilling the prediction that multiple autosomal factors are involved in the X-inactivation pathway. Our results indicate that the mutations target the X chromosome inactivation mechanism occurring in the embryo proper and do not affect the imprinted form of X-inactivation or genomic imprinting mechanisms. Further, we demonstrate through genetic analysis of mutant animals that are homozygous at the *Xce* locus that the effects of the X-inactivation mutations in both pedigrees are specific to animals that are heterozygous at the *Xce* locus. Together, the studies presented here are consistent with a model in which the mutations target factors in the X-inactivation pathway specifically involved in the choice or the initiation of X inactivation.

MATERIALS AND METHODS

Mice: C57BL/6J, BALB/cByJ, B6CBAF_1/J, and CAF1/J mice were purchased from The Jackson Laboratory and CD-1 mice were purchased from the Charles River Laboratory (Wilmington, MA). The tester stock of mice, containing *M. m. castaneus* (CAST/Ei) alleles along the length of the X chromosome on a 129S1/SvJ background, was generated as described (Plenge *et al.* 2000). The tester stock was maintained subsequently by brother-sister mating.

ENU mutagenesis: ENU was purchased (Sigma, St. Louis). Ten milliliters of 95% ethanol was injected into the Isopac container and 5 ml of the solution was discarded. To the remaining solution, 95 ml phosphate-citrate buffer (0.1 M Na_2HPO_4, 0.05 M NaCitrate, pH 5.0) was added. The ENU concentration was determined by spectrophotometry at 398λ and by applying the following formula: [ENU] = (OD_{398}/0.72) (5). The injection volume was calculated as follows: ml ENU = (dose/[ENU]) (grams body weight). ENU was injected intraperitoneally and doses requiring multiple injections were repeated weekly. The ENU doses, which ranged from a mini-

mum of 200 mg to a maximum of 400 mg, were administered as single treatments or as multiple (fractionated) treatments (Table 1). Animals treated with single large doses (200 or 250 mg) and animals treated with fractionated high doses (four doses of 100 mg each) fared the most poorly. In general, F_1 hybrid animals had a higher survival rate and recovered fertility faster than inbred BALB/cByJ animals treated with the same dose, consistent with previous studies (Russell *et al.* 1982; Favor 1988; Nolan *et al.* 1997; Justice *et al.* 1999; Weber *et al.* 2000). The time required to restore fertility to a particular male was measured from the date of the last injection. Female progeny of ENU-treated males, designated as G_1, were weaned at approximately 3 weeks of age. Because the primary screening phenotype—X inactivation—is female specific, male progeny were sacrificed. Matings were continued until ~50 female pups were generated from each male.

Embryo dissections: Embryos were dissected according to specifications described elsewhere (Hogan *et al.* 1994). First day after mating was designated 0.5 dpc (days post-coitum). Timed embryos were aged more specifically by morphology (Rugh 1994).

RNA isolation: Toe and ear samples were collected from each animal at weaning (~3 weeks of age). RNA from G_1 animals was isolated using the Purescript RNA isolation kit (Gentra Systems, Minneapolis) for 5- to 10-mg tissue samples according to the manufacturer's recommendations. Toe/ear and embryo RNA from animals of the G_2 and all subsequent generations was isolated using the HighPure RNA tissue kit (Roche Molecular Biochemicals) with minor modifications to the manufacturer's recommendations. Complete liver, kidney, heart, and tongue samples were collected. RNA was isolated from kidney, heart, and tongue using the NucleoSpin RNA II purification kit (CLONTECH, Palo Alto, CA) according to the manufacturer's recommendations. RNA was isolated from whole liver with the $LiCl_2$ isolation procedure as previously described (Auffray and Rougeon 1980). RNA samples from liver, kidney, heart, and tongue tissues were purified further for use in LightCycler assays by processing through the HighPure RNA tissue kit.

cDNA synthesis: Approximately 0.75 μg of RNA was reverse transcribed in a 20-μl reaction containing 10 mm dithiothreitol (GIBCO BRL, Gaithersburg, MD), 500 μm of each dNTP (GIBCO BRL), 1× first strand buffer (GIBCO BRL), 25 ng random primers (GIBCO BRL), 200 units of M-MLV RT (GIBCO BRL) and 20 units of RNaseOUT ribonuclease inhibitor (GIBCO BRL). Samples were incubated for 10 min at room temperature, 60 min at 37°, and 10 min at 95°. Specific-primed reverse transcription was carried out for embryo samples to be characterized with the *Xist* assay by substituting 10 pmol of the Xist-R 5′-CCGATGGGCTAAGGAGAAG-3′ primer for the random primer.

***Pctk1* and *Xist* allele-specific expression assay:** The *Pctk1* and *Xist* expression assays were conducted as previously described (Percec *et al.* 2002).

***H19* allele-specific expression assay:** The *H19* allele-specific expression assay was carried out as previously described (Thorvaldsen *et al.* 2002).

***Snrpn* allele-specific expression assay:** The *Snrpn* expression assay was conducted on cDNA using the LightCycler real time PCR system (Roche Molecular Biochemicals). *Snrpn* primers, Sn1 (5′-CTCCACCAGGAATTAGAGGC-3′) and Sn3 (5′-TATAGTTAATGCAGTAAGAGG-3′), were used to amplify a 155-bp region of the *Snrpn* gene (Szabo and Mann 1995). Fluorescence resonance energy transfer hybridization probes were designed to the C57BL/6 amplicon. The *Snrpn* sensor probe (5′-GAAGCATTGTAGGGGAAGAGAA-FL-3′) spans a single nucleotide polymorphism at nucleotide 915 between C57BL/6 (C) and CAST/Ei (T) and was labeled with fluorescein at the 3′ end. The *Snrpn* anchor probe (5′RED640-GGCTGAGATTTATCAACTGTATCTTAGGGTC-P3′; Idaho Technologies, Salt Lake City) was labeled with LC-Red640 at the 5′ end and was phosphorylated at the 3′ end. To a Ready-To-Go PCR bead (Amersham Biosciences), 5.12 μl H_2O, 0.38 μl TaqStart antibody (CLONTECH), and 1.5 μl 25 mm $MgCl_2$ (final concentration 3.0 mm) were added, and the reaction was incubated at room temperature for 5 min. After incubation, a final concentration of 12% DMSO, 0.5 μm of each primer, and 0.3 μm of each probe were added to the mix and the volume brought to 12.5 μl. From this reaction mix 10 μl was removed and added to a LightCycler glass capillary (Roche), and 10 μl cDNA and H_2O were added for a final reaction volume of 20 μl. After an initial denaturation step at 95° for 2 min, amplification was performed for 65 cycles at 95° for 1 sec, 50° for 15 sec, and 72° for 6 sec. A single fluorescence acquisition occurred at the end of each annealing step. After amplification, a final denaturation and annealing step was conducted (95° for 3 min, 35° for 2 min), followed by a melting curve analysis with fluorescence acquisition occurring continuously as the temperature was increased from 35° to 85° in 0.2° increments. After background subtraction, the contribution of each allele was calculated as the peak height of the melting curve generated at the allele-specific temperature, ~56.5° for C57BL/6 and 51° for CAST/Ei (LightCycler Data Analysis Software).

***Cdkn1c* allele-specific expression assay:** To a Ready-To-Go PCR bead, 0.3 μm of each primer and 1 μl of cDNA were added. Primers p576 (5′-CGGACGATGGAAGAACTCTGG-3′) and p574 (5′-TACACCTTGGGACCAGCGTACTCC-3′) amplified a 167-bp fragment (94° for 2 min followed by 35 cycles at 94° for 15 sec, 50° for 10 sec, and 72° for 20 sec) containing a polymorphism between C57BL/6 (T) and CAST/Ei (C; position 1256, MMU20553). The amplified product was digested with *Taq*I to reveal the CAST/Ei polymorphism (cleaved products are 118 and 49 bp) and resolved on a 7% polyacrylamide gel.

***Makorin3* allele-specific expression assay:** To a Ready-To-Go PCR bead, 0.3 μm of each primer and 1 μl of cDNA were added. Primers -Zf1 (5′-GACAGCCTTACCGAGGTCGC-3′) and Zf2 (5′-CATGGGGGTATGCACACCTG-3′) amplified a 215-bp C57BL/6 fragment and a 225-bp CAST/Ei fragment (94° for 2 min followed by 35 cycles at 94° for 15 sec, 55° for 10 sec, and 72° for 20 sec). Restriction digestion with *MspA1*I produces 152- and 67-bp bands for C57BL6/J cDNA while CAST/Ei cDNA remains uncleaved. The products were resolved on a 7% polyacrylamide gel.

Genotyping: All genotyping was carried out by PCR amplification of MIT microsatellite markers. For PCR amplification, ~100 ng of genomic DNA (or 1 μl of supernatant from the DNA isolation procedure) and 0.5 μm of each primer were added to a Ready-To-Go PCR bead (Amersham Pharmacia Biotech) according to the manufacturer's recommendations. After an initial denaturation step at 95° for 2 min, amplification was performed for 35 cycles at 95° for 15 sec, 55° for 10 sec, and 72° for 20 sec. Genotyping of the X chromosome was carried out routinely with *DXMit53* (~5 cM from *Pctk1*) and *DXMit18* (<1 cM from *Xist* and *Xce*) to determine genotypes at *Pctk1* and *Xist/Xce*, respectively. These markers are polymorphic between CAST/Ei and other inbred mouse strains.

RESULTS

X-inactivation pattern measured by allele-specific expression assays: We previously reported two mutant pedigrees segregating aberrant X-inactivation phenotypes (Percec *et al.* 2002) and here provide the details of

TABLE 1

ENU treatment regimen

Strain	Xce Genotype	No. of doses (mg ENU)	Total no. of mice	Total no. fertile	Offspring ≥2 SD	Offspring progeny tested	Offspring heritable mutations
BALB/cByJ	Xce^a	4 × (100)	10	0	0	0	0
		3 × (100)	15	8	7	2	1
		4 × (85)	15	1	0	0	0
		1 × (250)	5	0	0	0	0
		1 × (200)	5	1	0	0	0
$B6CBAF_1/J$	Xce^b	4 × (85)	30	24	21	4	2
		4 × (100)	10	2	0	0	0
CAF_1/J	Xce^a	4 × (85)	10	5	0	0	0

Three different strains of mice were injected with various doses of ENU. The dose reflects milligrams of ENU per gram of body weight. The total number of males injected is shown as well as the number that regained fertility after treatment. The founder male for female 24.21 is from the BALB/cByJ three-dose (100 mg) treatment group and the founder male for female 1.19 is from the $B6CBAF_1/J$ four-dose (85 mg) treatment group.

the original mutagenesis screen. To detect mutations specifically affecting the early steps of X chromosome inactivation, we screened for abnormalities in the X-inactivation pattern, a quantitative measure of cells that have chosen to keep one or the other X chromosome active. This phenotype reflects the X chromosome choice made by the population of progenitor cells undergoing inactivation during early embryogenesis. We hypothesized that screening for aberrations of the X-inactivation pattern would encourage the recovery of subtle mutations with primary effects on the X-inactivation pathway and possible secondary effects on genomic imprinting. To measure the X-inactivation pattern, we used an efficient quantitative allele-specific RT-PCR assay that measures transcript levels from the X-linked gene, *Pctaire-1* (*Pctk1*) in an allele-specific manner (Carrel *et al.* 1996; Plenge *et al.* 2000).

Nonrandom X chromosome choice occurs in the mouse when a "strong" *Xce* allele (*i.e.*, one that is more likely to be on the active X, such as the Xce^c allele derived from CAST/Ei mice) is inherited in combination with a "weak" allele (*i.e.*, one that is less likely to be on the active X, such as Xce^a or Xce^b derived from *M. m. domesticus* mice). The effect on the X-inactivation pattern exerted by the Xce^a and Xce^b alleles of various inbred mouse strains relative to the Xce^c allele derived from the CAST/Ei strain has been documented (Plenge *et al.* 2000). In these *Xce* heterozygous animals, ~25–30% of cells choose the X bearing the weaker *Xce* allele as the active X, instead of the 50% expected for a random process (Cattanach and Williams 1972; Cattanach and Johnston 1981; Johnston and Cattanach 1981; Rastan 1982; Cattanach and Rasberry 1994). The screen took advantage of this quantitative model of choice in which the effect of different *Xce* alleles is used as a baseline measure of the X-inactivation pattern. We hypothesized that the use of $Xce^{a/c}$ and $Xce^{b/c}$ heterozygotes (in contrast to *Xce* homozygotes) would facilitate the recovery of mutations disrupting general aspects of X chromosome choice as well as those specifically involved in *Xce* allelic discrimination.

ENU mutagenesis screen: Because we hypothesized that many unidentified factors must be involved in the pathway of X inactivation (Plenge *et al.* 2000), we screened for dominant mutations affecting the X-inactivation pattern. A total of 100 male mice were treated with ENU (Table 1). These consisted of 50 BALB/cByJ, 40 $B6CBAF_1/J$, and 10 CAF_1/J males. A total of 62% of the F_1 hybrid males recovered fertility after treatment with an average of 13 weeks of sterility. In contrast, only 20% of BALB/cByJ males recovered, after an average of 18 weeks of sterility. ENU-treated males that recovered fertility after treatment (G_0) were mated to females from a tester stock of mice selected to have a CAST/Ei X chromosome. BALB/cByJ and CAF_1 males possess an X chromosome bearing a Xce^a allele while $B6CBAF_1/J$ males possess an X chromosome bearing a Xce^b allele (Plenge *et al.* 2000). All female progeny (G_1) thus inherited a maternal CAST/Ei X chromosome and a paternal non-CAST/Ei X chromosome.

In total, we screened 84 $Xce^{a/c}$ and 252 $Xce^{b/c}$ G_1 female progeny of ENU-treated male mice (Percec *et al.* 2002). The former population represented the progeny of 10 BALB/cByJ and 5 CAF1 males and the latter represented the progeny of 26 $B6CBAF_1/J$ males that had recovered fertility after ENU treatment (Table 1). A maximum of 50 offspring were tested from each ENU-treated male to prevent the recovery of identical mutations from the limited population of spermatogonial stem cells (Justice *et al.* 1999; Weber *et al.* 2000). As described previously (Percec *et al.* 2002), the phenotypic distribution of the X-inactivation pattern in wild-type control females provided a statistical basis for screening the offspring of ENU-treated males and for discriminating between normal and aberrant phenotypes in the female progeny of ENU-treated males. We

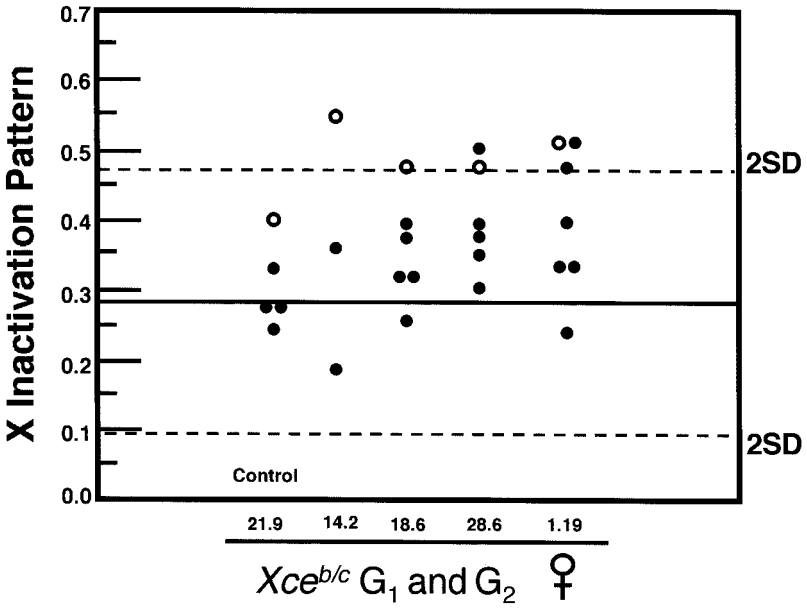

Figure 1.—Progeny test of $Xce^{b/c}$ candidate mutant females. Four affected $Xce^{b/c}$ G_1 females, 14.2, 18.6, 28.6, and 1.19, and one unaffected $Xce^{b/c}$ G_1 female, 21.9, serving as a negative control, (○) were progeny tested and their respective G_2 female progeny (●) are shown. The X-inactivation pattern was calculated with the *Pctk1* assay as the proportion of transcription from the X chromosome bearing the weaker *Xce* allele to the total transcription from both X chromosomes. The mean for the respective wild-type *Xce* heterozygous distribution is depicted by a solid horizontal line and the two standard deviations from the mean of the wild-type population are depicted by dashed horizontal lines.

considered any G_1 animals with X-inactivation patterns ≥2 standard deviations (SD) from the mean of the wild-type population candidates for X-inactivation mutants. To avoid recovery of X-linked mutations unrelated to primary effects on X-inactivation choice, we focused on animals that preferentially maintained the mutagenized X chromosome as the active X.

Two $Xce^{a/c}$ and four $Xce^{b/c}$ G_1 females fulfilling the candidate mutant criteria were progeny tested (data not shown and Figure 1) to exclude statistical variants from further analysis. It is recognized that some true mutants may have been excluded, such as those with mutations of low penetrance, with maternally imprinted effects, with transmission ratio distortion, or those missed simply because of inadequate numbers of informative offspring (less than half of the female progeny were heterozygous at both the *Pctk1* and *Xce* loci). As expected, the phenotyping control female (21.9) transmitted only wild-type X-inactivation patterns to her progeny. Three of the six candidate females tested (23.14, 14.2, and 18.6) were classified into the statistical variant category (data not shown and Figure 1). Significantly, however, three G_1 females (24.21, 1.19, and 28.6) transmitted aberrant X-inactivation patterns to a subset of their female offspring, consistent with the segregation of a dominant mutation (data not shown and Figure 1). (Given the nature of the quantitative cutoff used in this screen, each offspring with an X-inactivation pattern >2 SD above the mean has only a 2.5% probability of having that pattern by chance.) Candidate mutations segregating in the three animals were induced independently of one another, as these animals were the progeny of different ENU-treated founder males, with female 24.21 as the daughter of an ENU-treated BALB/cByJ male, and females 1.19 and 28.6 as the daughters of two ENU-treated $B6CBAF_1/J$ males. We investigated further one female from each *Xce* genotype and genetic class and thus examined females 24.21 and 1.19 as candidate mutants of X chromosome inactivation.

Establishment of the mutant phenotypes: To confirm and characterize further the phenotypes of the two candidate mutants, the *Xist* gene was assayed as a marker of X chromosome activity instead of the *Pctk1* gene used for the primary mutagenesis screen. Because phenotyping required heterozygosity at the locus assayed (originally *Pctk1*) and at *Xce*, a greater number of informative animals were generated when *Xist*, a marker tightly linked to *Xce*, was used for the allele-specific expression analysis. The *Xist* assay was applied to control unmutagenized $Xce^{a/c}$ and $Xce^{b/c}$ females to establish wild-type phenotypic parameters. The X-inactivation pattern in 55 wild-type $Xce^{a/c}$ females was normally distributed with a mean of 0.29 and an SD of 0.07 (Figure 2A). The X-inactivation pattern in 44 wild-type $Xce^{b/c}$ females also was normally distributed with a mean of 0.32 and an SD of 0.06 (Figure 2B). As expected, the phenotypic distributions were similar to those observed with the *Pctk1* assay (Percec *et al.* 2002). Phenotyping of several generations of control animals outcrossed to the tester stock confirmed that the X-inactivation pattern does not vary with segregation of the genetic background (Figure 2, A and B), consistent with prior studies (Plenge *et al.* 2000). The molecular phenotyping criteria for the *Xist* assay were designated in the same manner as they were for the *Pctk1* assay: affected females were defined by phenotypes that were ≥2 SD above the mean of the respective wild-type *Xce* genotypes. Carrier animals (males or females) are defined as those that have transmitted the mutant phenotypes to two or more female offspring. (The likelihood of such transmission occurring by chance is <0.001.)

To confirm heritability and to characterize further

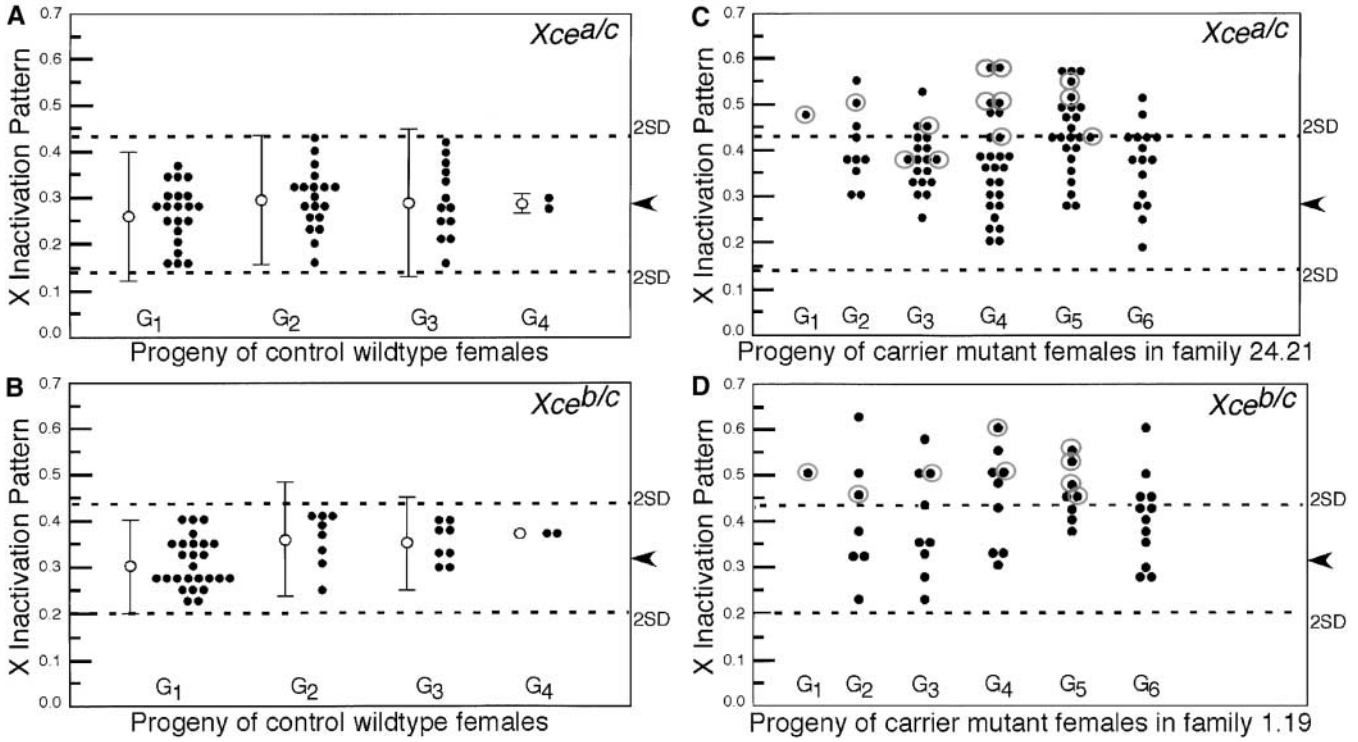

FIGURE 2.—Multigeneration progeny tests of wild-type and mutant animals. For the progeny test, females from each generation were bred to tester males and all informative (heterozygous at *Xist* and *Xce*) female progeny were phenotyped. *Xist* phenotyping of four generations of $Xce^{a/c}$ (A) and $Xce^{b/c}$ (B) unmutagenized control animals demonstrated that the X-inactivation phenotype remains constant despite outcrossing to the tester stock. For each control generation, an open circle and vertical bar depict the X-inactivation pattern mean and 2 SD demarcation, respectively. Transmission of the aberrant phenotype is demonstrated here in a dominant manner through the sixth generation in family 24.21 (C) and family 1.19 (D). In C and D, circled animals were progeny tested and gave rise to the subsequent generation. An arrowhead depicts the mean for the respective wild-type *Xce* heterozygous distribution and the dashed horizontal lines demarcate values within 2 SD from the mean of the wild-type populations. The X-inactivation pattern was calculated with the *Xist* assay as the proportion of transcription from the X chromosome bearing the stronger *Xce* allele to the total transcription from both X chromosomes.

the inheritance pattern of the mutant phenotypes from candidate mutant G_1 females 24.21 and 1.19, we phenotyped all informative female progeny generated throughout their lifetime (Figure 2, C and D). Affected females (defined as above) examined from both families transmitted the mutant phenotypes to the subsequent generation in a dominant manner. Both families stably segregated the mutant X-inactivation patterns through at least the seventh generation, G_7 (Figure 2, C and D, and data not shown). Carrier females from both pedigrees displayed X-inactivation patterns significantly different from those predicted by their respective *Xce* genotypes, as the X chromosome bearing the "weaker" *Xce* allele was the active X in a significantly higher than expected proportion of cells (compare Figure 2A to 2C and Figure 2B to 2D). The mean X-inactivation pattern of transmission-confirmed carrier females segregating in family 24.21 is 0.48 with a standard deviation of 0.07 while in family 1.19 these values are 0.51 and 0.04, respectively (Figure 2, C and D).

Mutant phenotype from family 1.19 segregates with two independent autosomal loci: Previous genetic segregation and mapping analysis demonstrated that the mutations segregating in both pedigrees map to autosomal loci and, more specifically, that mutation from family 24.21 maps to chromosome 15 (PERCEC *et al.* 2002). To localize the mutation in pedigree 1.19, four affected and transmission-tested females and five unaffected distantly related females from the fifth (G_5) and sixth (G_6) generations were genotyped with 81 informative microsatellite markers evenly spaced across the genome with a maximum swept radius of 30 cM (Figure 3 and data not shown). Informative markers were selected that distinguish ENU-treated alleles C57BL/6J and CBA/J from wild-type 129S1/SvJ and CAST/Ei alleles. Alleles from the mutagenized $B6CBAF_1/J$ founder male were observed at the expected frequency, ~2.8 and 1.2% in unaffected G_5 and G_6 animals, respectively (as compared to the expected 1/32 or 3% and 1/64 or 1.5% of alleles in wild-type G_5 and G_6 animals, respectively), serving as genotyping controls (data not shown). No regions of the genome exhibited nonrandom segregation of any markers in the unaffected females tested. In affected females, however, two regions of the genome, distal 23 cM of chromosome 5 and ~30 cM of the proximal chromosome 10, demonstrated significant linkage ($P <$

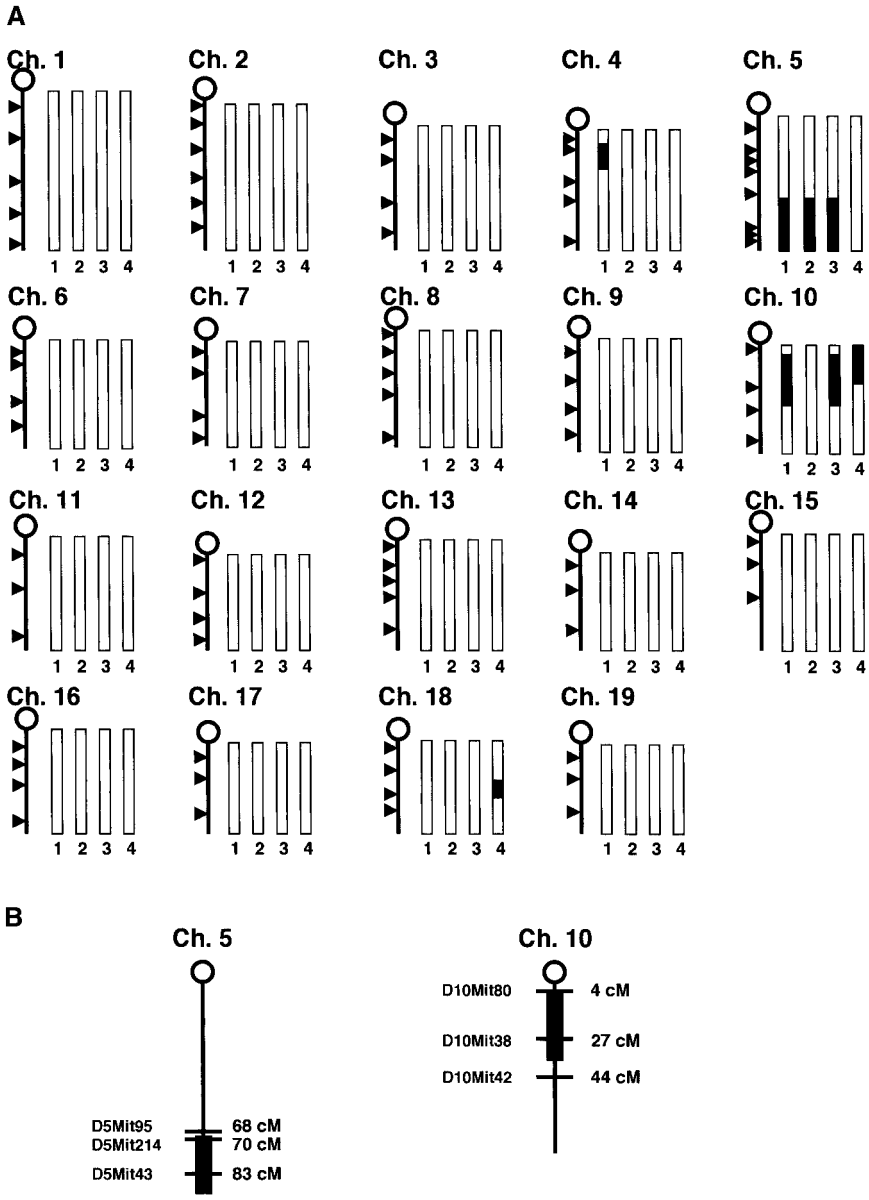

FIGURE 3.—Genome scan of family 1.19 localizes mutant phenotype to chromosomes 5 and 10 (A). Four affected G_5 (4) and G_6 (1–3) females were genotyped with 81 microsatellite markers spaced evenly throughout the genome with a maximum spacing of 30 cM. Arrowheads on the left of each chromosome designate the location of the markers. Genotypes for the four individual females are represented as vertical bars 1–4 for each chromosome. Open regions of the bars represent wild-type genotypes (*i.e.*, from the nonmutagenized parent), while solid regions represent C57BL/6J or CBA/J alleles inherited from the ENU-treated founder male. The probability that the ENU-treated alleles were inherited by chance in the regions of chromosome 5 and chromosome 10 is $P < 0.03$. Mapping of chromosomes 5 and 10 (B) suggests that the mutations are located within the distal 23 cM of chromosome 5 and within a 30-cM region of the proximal chromosome 10. The MIT microsatellite markers used for genotyping are designated at the left of each chromosome with the approximate Mouse Genome Database (MGD) genetic map location shown on the right. The map locations of markers employed for this genotyping were consistent between the MGD, Ensemble, and Celera databases.

0.03) to the mutant phenotype, calculated as the probability of random segregation of the mutant C57BL/6J and CBA/J alleles to the animals tested (Figure 3B). The results of the genome scan indicate that two regions of the genome are segregating with the mutant phenotype in pedigree 1.19.

To determine definitively whether one or both candidate regions are responsible for the mutant phenotype, we progeny-tested animals carrying both candidate regions, as well as animals carrying one or the other candidate regions (Table 2, Figure 4, and data not shown). Animals carrying both regions clearly transmitted the mutant phenotype to offspring (Figure 4, A and B). Significantly, animals carrying solely the candidate region on chromosome 10 transmitted the mutant phenotype to their offspring in a dominant manner, indicating that there is a mutation in this region that is sufficient to induce the aberrant X-inactivation pattern (Figure 4C). Furthermore, animals carrying solely the candidate region on chromosome 5 also transmitted the mutant phenotype to their offspring in a dominant manner, indicating that there is a mutation in this region as well that is sufficient to induce the aberrant X-inactivation pattern (Figure 4D). These data suggest that two independent mutations are segregating in this pedigree and that each of the two mutations is sufficient to cause the mutant X-inactivation phenotype. The changes in the X-inactivation pattern induced by each mutation were quantitatively similar to one another as well as to the mutant phenotype exhibited by double heterozygotes, indicating that any additive effect on the phenotype is likely to be subtle. In addition, the phenotypes of each of the two mutations were similar when transmitted independently through male and female lines, sug-

TABLE 2

Candidate region segregation in transmission-proven carrier animals from family 1.19

Generation	XCI	Chromosome 5 candidate region	Chromosome 10 candidate region	Sex
1	0.50	+	+	F
2	0.46	+	+	F
3	0.51	+	+	F
3	NA	+	−	M
3	NA	−	+	M
4	0.55	+	+	F
4	0.54	+	+	F
4*	0.42	−	+	F
4	NA	−	+	M
5	0.52	+	−	F
5	0.54	+	+	F
5	0.45	+	+	F
5*	0.50	−	+	F
5*	0.51	−	+	F
6	0.50	+	+	F
6	NA	−	+	M

Representative progeny-tested male (M) and female (F) animals from different generations of family 1.19 carrying either both candidate regions on chromosomes 5 and 10 or one or the other candidate regions transmitted the mutant phenotype to their offspring in a dominant manner. Each row depicts the data from a single progeny-tested animal. The X-inactivation phenotype at the *Xist* locus (XCI) is shown for each female tested. Male carriers cannot be assayed directly for X inactivation (NA). For each animal, the presence (+) or absence (−) of the mutant genotype at the candidate regions on chromosomes 5 and 10 is shown. These females are not represented in Figure 2D. These data suggest that two independent mutations are segregating in this pedigree and that each of the two mutations is sufficient to cause the mutant X-inactivation phenotype. *Females that are derived from carrier males.

gesting that the mutant factors are not subject to an imprinting effect (Table 2, Figure 2D, Figure 4, and data not shown).

Mutant phenotypes do not perturb imprinted X inactivation in family 24.21: The analysis of the mutant X-inactivation phenotypes in families 24.21 and 1.19 has thus far been limited to somatic tissues including adult tissues and tissues of the embryo proper. X inactivation in extraembryonic tissues of the mouse differs, however, from its somatic counterpart by undergoing paternally imprinted X inactivation (Takagi and Sasaki 1975; Huynh and Lee 2001). To determine whether the mutations in our families also affect the imprinted form of inactivation, we examined the X-inactivation pattern in extraembryonic tissues of early embryos with the *Xist* assay (Table 3). Because the *Xce* locus does not affect X chromosome choice in extraembryonic tissues, we phenotyped *Xce* heterozygous embryos (Takagi and Sasaki 1975; Rastan and Cattanach 1983). In extraembryonic tissues of wild-type 8.5- and 10.5-dpc embryos, we observed exclusive expression of *Xist* from the paternal allele, consistent with paternal-specific silencing of the

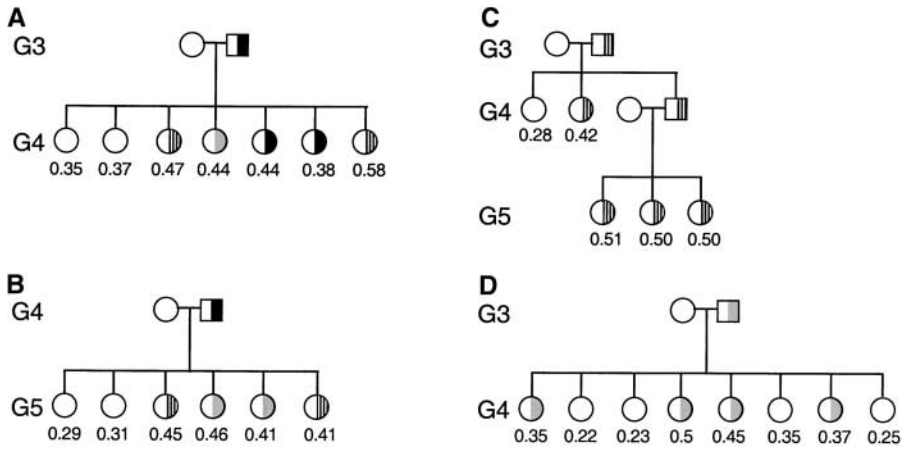

Figure 4.—Partial pedigrees of family 1.19 depict phenotype-genotype associations in animals carrying candidate regions on chromosomes 5 and 10 (A and B), animals carrying solely the candidate region on chromosome 10 (C), and animals carrying solely the candidate region on chromosome 5 (D). Circles represent females and squares represent males. Half-solid symbols represent animals carrying both chromosome 5 and 10 candidate regions, half-shaded symbols represent animals carrying only the chromosome 5 candidate region, half-striped symbols represent animals carrying only the chromosome 10 candidate region, and open symbols represent animals carrying neither candidate region. The XCI pattern is noted below each animal. These data suggest that the two mutations segregate independently in this pedigree and that each mutation is sufficient to cause the mutant X-inactivation phenotype.

TABLE 3

Imprinted X inactivation in extraembryonic tissues of embryos of family 24.21

Stage	Animal	*N*	XCI embryo	XCI EE tissues
8.5 dpc	Control	1	0.35	Paternal
8.5 dpc	24.21	7	0.37–0.51	Paternal
9.5 dpc	24.21	6	0.4–0.55	Paternal
10.5 dpc	Control	2	0.3–0.32	Paternal

The X chromosome inactivation phenotype (XCI) at the *Xist* locus in *Xce* heterozygous wild-type embryos and in embryos from family 24.21 demonstrated complete paternal X inactivation (as demonstrated by >90% paternal *Xist* expression) in extraembryonic (EE) tissues, ectoplacental cone (8.5 dpc), and placental tissues (9.5 and 10.5 dpc). The number of embryos tested from each category is shown (*N*). The X-inactivation phenotype at the *Xist* locus is shown in embryonic tissues of the respective animal. When more than one embryo was tested from a given category, the X chromosome inactivation phenotype (XCI) is shown as the range of phenotypes from the respective group. Genotyping of the candidate region on chromosome 15 in embryos from family 24.21 determined that all of the tested embryos carry the candidate region.

X chromosome. In extraembryonic tissues of 8.5- and 9.5-dpc embryos from family 24.21, we also observed exclusive expression of *Xist* from the paternal allele, indicating that paternal imprinting is not perturbed by the mutation segregating in family 24.21.

Mutant phenotypes do not perturb genomic imprinting: To maintain and perhaps initiate X chromosome silencing, the X-inactivation pathway employs factors that are common to other epigenetic processes, including genomic imprinting. Therefore, it is possible that the factors targeted by our candidate mutations may be common to multiple epigenetic silencing pathways. To address this directly, we inquired whether the candidate mutations affect genomic imprinting of the well-characterized *H19, Snrpn, Cdkn1c* (*p57^{kip2}*), and *Makorin3* (*Zfp127*) genes (Bartolomei *et al.* 1991; Leff *et al.* 1992; Hatada and Mukai 1995; Jong *et al.* 1999). *H19* and *Cdkn1c* normally are expressed only from the maternal allele while *Snrpn* and *Makorin3* are expressed only from the paternal allele. Affected and unaffected females from both pedigrees were examined with allele-specific expression assays and all exhibited appropriate imprinting (Table 4). For the analysis of family 1.19, we examined double heterozygous animals that carried both chromosome 5 and chromosome 10 mutations. These observations indicate that genomic imprinting is not perturbed by any of the three mutations segregating in the two pedigrees.

Mutant phenotypes in *Xce* homozygous females: The mutant phenotypes in families 24.21 and 1.19 have been defined by their effect on the X-inactivation pattern in *Xce* heterozygous animals. Because the mutant phenotypes shift the X-inactivation pattern from the wild-type nonrandom inactivation choice characteristic of *Xce$^{a/c}$* and *Xce$^{b/c}$* genotypes to a phenotype closer to the random X-inactivation pattern characteristic of *Xce* homozygotes (Plenge *et al.* 2000), we asked whether the mutant effects can be detected in the X-inactivation pattern in *Xce* homozygotes from the two pedigrees by measuring the X-inactivation pattern in *Xce* homozygous female progeny of *Xce* heterozygous carriers.

For this analysis, phenotyping of the two families was conducted by assaying the *Pctk1* gene as a marker of X chromosome activity. The *Pctk1* assay was employed since *Xist* and *Xce* are tightly linked and both loci would be homozygous in these animals. The *Pctk1* assay was applied first to wild-type control *Xce$^{c/c}$* females to establish wild-type phenotypic parameters for the assay, including mean and standard deviations (Figure 5). All categories of *Xce* homozygous females (*i.e.*, *Xce$^{c/c}$*, *Xce$^{a/a}$*, and *Xce$^{b/b}$*) are expected to display random X-inactivation patterns (Plenge *et al.* 2000). As predicted, the X-inactivation pattern in nine wild-type *Xce$^{c/c}$* females tested was normally distributed with a mean of 0.5 and an SD of 0.07, consistent with previous studies (Plenge *et al.* 2000). This phenotypic distribution therefore may be applied to the comparison of all classes of *Xce* homozygotes.

The X-inactivation pattern was characterized in the *Xce* homozygous female progeny of carrier females from both families. Again, the animals examined from family 1.19 were double heterozygous animals that carried both chromosome 5 and chromosome 10 mutations. The mean X-inactivation pattern in *Xce$^{c/c}$* females tested from families 24.21 and 1.19 did not differ significantly from the wild-type *Xce$^{c/c}$* population (Figure 5). Further, the X-inactivation pattern in *Xce$^{a/a}$* female progeny of carrier females from family 24.21 did not differ from the wild-type *Xce$^{c/c}$* population (Figure 5). In contrast, the variance differed significantly between the two 1.19 and control groups ($P = 0.02$). This difference is not observed between the 24.21 and control groups, which suggests that the mutations in the two pedigrees may act via different mechanisms to induce the aberrant X-inactivation phenotypes. As additional confirmation of the *Xce* homozygous phenotypes in adult tissues, the X-inactivation pattern was characterized in *Xce* homozygous wild-type control and mutant embryos from pedigree 24.21 (data not shown). As expected, both wild-type and mutant embryos displayed random X-inactivation patterns that were similar to one another as well as to those observed in mutant *Xce* heterozygous embryos of the same family. These data suggest that the candidate mutations from both families may have targeted factors specifically involved in X chromosome choice and in *Xce* allelic discrimination.

DISCUSSION

ENU mutagenesis for subtle molecular phenotypes: To advance the understanding of epigenetic regulatory mechanisms, we conducted a dominant, genome-wide,

TABLE 4

Imprinting in affected and unaffected females from families 24.21 and 1.19

Animal	XCI	*H19* expression	*Cdkn1c* expression	*Snrpn* expression	*Makorin3* expression
24.21 affected	0.43	Maternal	ND	ND	ND
24.21 affected	0.50	Maternal	Maternal	Paternal	Paternal
24.21 unaffected	0.29	Maternal	Maternal	Paternal	Paternal
24.21 unaffected	0.29	Maternal	ND	ND	ND
24.21 unaffected	0.26	Maternal	Maternal	Paternal	Paternal
1.19 affected	0.50	Maternal	ND	ND	ND
1.19 affected	0.44	Maternal	Maternal	Paternal	Paternal
1.19 affected	0.60	Maternal	Maternal	Paternal	Paternal
1.19 unaffected	0.22	Maternal	ND	ND	ND
1.19 unaffected	0.31	Maternal	ND	ND	ND

Genomic imprinting at the *H19, Snrpn, Cdkn1c,* and *Makorin3* loci was assayed with allele-specific expression assays in unaffected and affected females from both families. Appropriately imprinted monoallelic expression was observed for all loci in all animals tested (as demonstrated by >95% expression from the expected allele). For comparison, the X-inactivation phenotype (XCI) at the *Xist* locus is shown for each animal. ND refers to animals that were not assayed. In most cases, animals were not assayed because they were homozygous at the locus of interest.

phenotype-driven ENU mutagenesis screen to detect novel regions of the mouse genome involved in X chromosome inactivation and hypothesized that this approach would result in a high rate of novel mutation detection, given the paucity of genes currently known in the pathway and the likelihood that many more genes are involved. Two recent large-scale studies demonstrated dominant mutation frequencies as high as 2% when a spectrum of phenotypes was screened for mutations, with >50% of the abnormal phenotypes detected in the screen resulting from heritable mutations (Habre de Angelis *et al.* 2000; Nolan *et al.* 2000). Small-scale ENU mutagenesis screens focusing on morphological phenotypes have proven to be as successful as the larger studies, if not more so (Kasarskis *et al.* 1998; Hentges *et al.* 1999). The estimated minimum mutation frequency for our screen, 0.9% (3/346), is within the range of these latest parameters. Because not all females with abnormal X-inactivation phenotypes were characterized genetically, it is not known whether additional females carried heritable mutations; thus, our estimated mutation frequency is likely an underestimate.

Our results clearly demonstrate that small-scale ENU mutagenesis screens can be applied successfully to the recovery of multiple mutations resulting in subtle molecular phenotypes. The use of high fractionated ENU doses and a sensitive and robust assay, and the likelihood that many factors are involved in the epigenetic control of the X-inactivation pathway, contributed to the successful recovery of mutants in our screen. These observations indicate that many other molecular pathways would be amenable to genetic dissection through the use of small-scale ENU mutagenesis screens if screening parameters were carefully optimized. While other ENU mutagenesis screens have attempted to identify mutations involved in epigenetic factors (Tsai *et al.* 2001), fewer mutations have been detected from this type of screen than from screens for other developmental phenotypes. Presumably, this is due to the lethal nature of severely abnormal epigenetic phenotypes. Thus, the recovery of epigenetic mutations may be enhanced by the use of highly quantitative screening assays such as the one applied in our screen.

Mutant phenotypes are specific to X chromosome inactivation: The mutant phenotypes segregating in our pedigrees could result from mutations in global factors, such as housekeeping genes, or from mutations in factors specific to the X-inactivation pathway. In the former scenario, the mutant phenotypes would be manifested in both sexes and affect multiple developmental and genetic pathways. Such mutations may have targeted factors involved in epigenetic silencing mechanisms common to both X inactivation and genomic imprinting. Our data demonstrate intact genomic imprinting of four different imprinted genes in carrier females from both families, indicating that none of the mutations has targeted a factor essential to the epigenetic regulation of genomic imprinting. Consequently, our studies present no evidence for any effect of the candidate mutations beyond the X-inactivation pattern, suggesting that the mutations have targeted factors specific to the pathway of X inactivation.

Mutant phenotype of family 24.21 does not affect imprinted X inactivation: Previous studies of early postimplantation embryos from both families established that the mutant X-inactivation phenotypes are manifested early in development around the time that X inactivation occurs (Percec *et al.* 2002). The mutant phenotypes characterizing the early postimplantation embryos were similar to those observed in adult siblings,

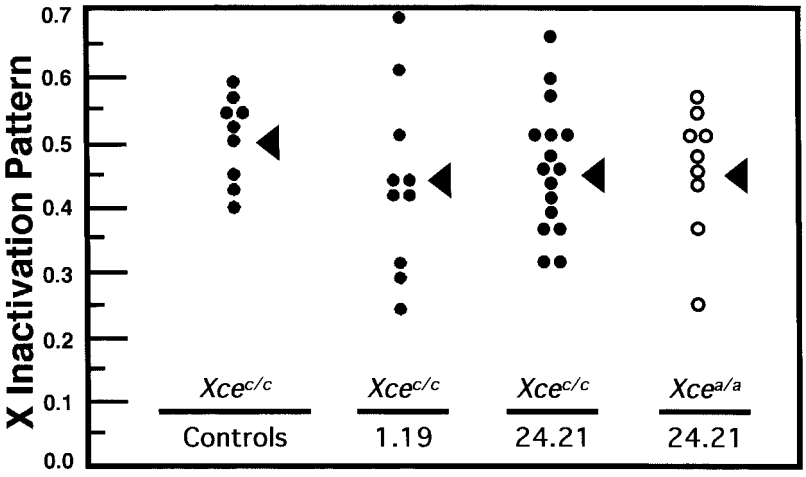

FIGURE 5.—Mutant X-inactivation phenotype in *Xce* homozygous females from both families. The X-inactivation phenotype at the *Pctk1* locus in adult $Xce^{c/c}$ wild-type control females, in $Xce^{c/c}$ homozygous female progeny of family 1.19 carrier females, in adult $Xce^{c/c}$ (●), and in adult $Xce^{a/a}$ (○) female progeny of family 24.21 carrier females. An arrowhead depicts the mean X-inactivation pattern for each group. The $Xce^{a/a}$ and $Xce^{c/c}$ homozygous females from family 24.21 have the same mean. The X-inactivation pattern was measured with the *Pctk1* assay.

indicating that the phenotypes are well established prior to the developmental stages studied. While the X-inactivation pattern in somatic tissues of the embryo and adults is clearly affected by the mutations in both pedigrees, imprinted inactivation of the paternal X chromosome in extraembryonic tissues is not affected in family 24.21. These results indicate that the mutation in family 24.21 specifically affects the random (embryonic) form of X inactivation.

Genetic composition of the candidate mutations in family 1.19: The identification of two regions of the genome that segregate independently with the mutant phenotype in family 1.19 raised the possibility that genetic modifiers may contribute to the mutant phenotype in this family. The prospect that a modifier is involved is especially noteworthy, as alleles from four different mouse strains [composed of two ENU-treated genomes, C57BL/6J and CBA/J (from the $B6CBAF_1/J$ founder), and the wild-type 129S1/SvJ and CAST/Ei genomes] segregate in this pedigree. C57BL/6J alleles segregate in the candidate region of chromosome 10 while CBA/J alleles segregate in the candidate region of chromosome 5. The multiple genetic strains segregating in this family may have encouraged the interaction of genetic modifiers between two strains or between an ENU-induced mutation and a modifier in the ENU-treated strain. While we cannot rule out that any of the candidate intervals in both pedigrees contain strain-specific modifiers rather than ENU-induced mutations, the identification of novel autosomal genes in the X-inactivation pathway is equally significant, whether resulting from the activity of modifiers or from ENU-induced mutations.

Candidate genes that are likely to be involved in the pathway of X chromosome inactivation include those that affect epigenetic silencing mechanisms through the modification of chromatin structure and function. Among such candidate genes on the distal interval of chromosome 5 are zinc-finger protein 70 (*Zfp70*), high mobility group box 1 (*Hmgb1*), breast cancer 2 (*Brca2*), heat-shock protein 25 kD (*Hsp25*), and zinc-finger proliferation 1 (*Zipro1*). Candidate genes on chromosome 10 include BRCA2-associated factor 35 (*Braf35*), histone deacetylase 2 (*Hdac2*), methyl CpG-binding domain protein 3 (*Mbd3*), DNA methyltransferase 3l (*Dnmt3l*), and zinc-finger protein, autosomal (*Zfa*). Candidate genes in the previously mapped pedigree 24.21 include RAD21 homolog (*Rad21*), zinc fingers and homeoboxes protein 1 (*Zhx1*), and KH-domain-containing, RNA-binding, signal-transduction-associated 3 (*Khdrbs3*) on chromosome 15. Significantly, the candidate regions do not contain known genes for factors previously shown to be involved in any aspect of X inactivation, indicating that the mutations segregating in pedigrees 1.19 and 24.21 affect novel factors in the X-inactivation pathway.

Models of mutation activity: The results of the mutant phenotyping data presented here clearly delineate the effect of the mutations and are consistent with models in which the candidate mutations target specific factors in the X-inactivation pathway. Furthermore, our genetic analysis of mutant animals bearing selected *Xce* alleles establishes that the effect of the mutant phenotypes is exclusive to the X-inactivation mechanism in *Xce* heterozygous animals that undergo nonrandom X chromosome choice.

A variety of models may be invoked to explain the effect of the mutations segregating on mouse chromosomes 15, 5, and 10, designated X-inactivation autosomal factor 1, 2, and 3 (*Xiaf1, Xiaf2*, and *Xiaf3*), respectively. In both pedigrees, the X-inactivation pattern in carrier *Xce* heterozygous females is shifted away from the nonrandom X-inactivation pattern of wild-type *Xce* heterozygous females toward a more random X-inactivation pattern. The simplest explanation for this change is a defect in *Xce* allelic discrimination. Consequently, one or all candidate mutations may affect (different) factors involved in distinguishing *Xce* alleles during X chromosome selection (Figure 6). It has long been hypothesized that during initiation of X chromosome silencing an autosomally encoded dosage-sensitive block-

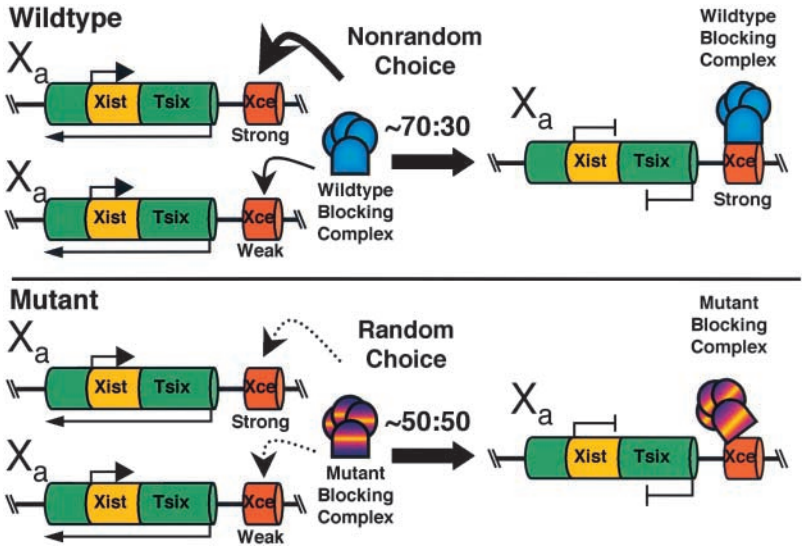

FIGURE 6.—Model of mutation activity. During X chromosome selection in wild-type *Xce* heterozygotes, a dosage-sensitive, autosomally encoded *Xic* blocking complex preferentially recognizes the stronger *Xce* allele, maintaining its activity and resulting in a nonrandom X-inactivation pattern. In pedigrees 24.21 and 1.19, autosomal-dominant mutations may lead to conformational change or to haplo-insufficiency of a factor within the mutant blocking complex. According to this model, the mutations abrogate preferential activity of the blocking complex and result in partial reversion to random X chromosome choice.

ing complex protects one *Xic* from inactivation (perhaps through action at the *Xce* locus), thereby choosing that chromosome to remain active (RUSSELL 1963; BROWN and CHANDRA 1973; RUSSELL and CACHEIRO 1978; AVNER and HEARD 2001). It is not known how the distinction of *Xce* alleles in an *Xce* heterozygous animal occurs, although differential methylation, CTCF binding, and chromatin structure may play a role (SIMMLER *et al.* 1993; AVNER *et al.* 1998; PRISSETTE *et al.* 2001; CHAO *et al.* 2002). In wild-type *Xce* heterozygotes, preferential interaction of the blocking complex with the stronger *Xce* allele (*e.g.*, the Xce^c allele) would result in nonrandom X-inactivation patterns (Figure 6). It is possible that the loci targeted by our mutations encode or affect members of the putative blocking complex and/or other autosomal factors that interact with *Xce*. The mutations described here, for example, may disrupt the ability of the blocking factor to differentiate between *Xce* alleles, resulting in a reversion to random (*i.e.*, ~50:50) X chromosome choice in mutant animals despite heterozygosity at *Xce*.

In an alternative model, the shift in the X-inactivation pattern in carrier *Xce* heterozygous females may not represent a change toward random X chromosome choice, but rather an increase in the variance of the X-inactivation pattern (NESBITT 1971). In this scenario, the candidate mutations may cause initiation and/or stabilization of X inactivation at an earlier stage when fewer cells are present in the embryo. In a parallel scenario, it is possible that the mutations may disrupt the stability of the inactivation choice such that a cell may no longer be able to "lock-in" X chromosome choice and thereby manifest a more random X-inactivation pattern. According to this model, the initiation step of the X-inactivation pathway may be affected by the mutation(s) with the other steps of the pathway proceeding normally, implicating as candidates any factors involved in the initiation of X inactivation. This includes RNA-binding molecules that may interact directly with the *Xist* or *Tsix* transcripts or molecules involved in chromatin structure, such as those that stabilize or lock in the inactive state during the shift from reversible to irreversible inactivation (WUTZ and JAENISCH 2000). Finally, it remains formally possible that the mutations lead to haplo-insufficiency of a dosage-sensitive factor involved early in the inactivation pathway, thereby resulting in altered X-inactivation patterns. Positional cloning and characterization of the three *Xiaf* genes identified here will be required to discriminate among these or other models.

Conclusion: Our study of ENU-induced mutations of X chromosome inactivation has identified three mutations that act early in development in an autosomal-dominant manner to induce X-inactivation patterns in *Xce* heterozygous animals that are significantly different from those predicted by their *Xce* genotypes. The mutations do not affect the X chromosome inactivation pattern in *Xce* homozygous animals, indicating that they may have targeted factors involved in *Xce* allelic discrimination during the X chromosome choice process. Significantly, neither imprinted X inactivation nor genomic imprinting is perturbed in mutant animals. Consequently, the phenotypic analyses presented here are consistent with models in which the mutations have affected molecules involved specifically in the choice or initiation steps of the X-inactivation pathway. Through our genomic mapping analysis of the two pedigrees we have shown that at least three novel autosomal loci are involved in the pathway of X inactivation, as none of the candidate regions harbor genes known to be involved in the process of inactivation. The identification of factors targeted by these mutations and other epigenetic muta-

tions detected through such ENU mutagenesis screens should play a significant role in our understanding of epigenetic regulation of the mammalian genome.

We thank Monica Justice and Jim Amos-Landgraf for helpful assistance with mutagenesis; Warren Ewens, David Beier, and Richard Spielman for statistical advice; Mellissa Mann for assistance with the *Snrpn* assay and the *Makorin3* and *Cdkn1c* polymorphisms; and Keith Olszens for animal husbandry and dissections. We also appreciate helpful discussions and critical reading of the manuscript by Maja Bucan. This work was supported by National Institutes of Health (NIH) grant GM-45441 (H.F.W.) and by the Howard Hughes Medical Institute (M.S.B.). I.P. was supported by an NIH Radiation Biology predoctoral training grant.

LITERATURE CITED

Auffray, C., and F. Rougeon, 1980 Purification of mouse immunoglobulin heavy-chain messenger RNAs from total myeloma tumor RNA. Eur. J. Biochem. **107:** 303–314.

Avner, P., and E. Heard, 2001 X-chromosome inactivation: counting, choice and initiation. Nat. Rev. **2:** 59–67.

Avner, P., M. Prissette, D. Arnaud, B. Courtier, C. Cecchi *et al.*, 1998 Molecular correlates of the murine *Xce* locus. Genet. Res. **72:** 217–224.

Bartolomei, M. S., S. Zemel and S. M. Tilghman, 1991 Parental imprinting of the mouse *H19* gene. Nature **351:** 153–155.

Boumil, R. M., and J. T. Lee, 2001 Forty years of decoding the silence in X-chromosome inactivation. Hum. Mol. Genet. **10:** 2225–2232.

Bourc'his, D., G. L. Xu, C. S. Lin, B. Bollman and T. H. Bestor, 2001 Dnmt3L and the establishment of maternal genomic imprints. Science **294:** 2536–2539.

Brockdorff, N., A. Ashworth, G. F. Kay, P. Cooper, S. Smith *et al.*, 1991 Conservation of position and exclusive expression of mouse *Xist* from the inactive X chromosome. Nature **351:** 329–331.

Brown, S. W., and H. S. Chandra, 1973 Inactivation system of the mammalian X chromosome. Proc. Natl. Acad. Sci. USA **70:** 195–199.

Brown, C. J., A. Ballabio, J. L. Rupert, R. G. Lafreniere, M. Grompe *et al.*, 1991 A gene from the region of the human X inactivation centre is expressed exclusively from the inactive X chromosome. Nature **349:** 38–44.

Carrel, L., C. M. Clemson, J. M. Dunn, A. P. Miller, P. A. Hunt *et al.*, 1996 X inactivation analysis and DNA methylation studies of the ubiquitin activating enzyme E1 and PCTAIRE-1 genes in human and mouse. Hum. Mol. Genet. **5:** 391–401.

Cattanach, B. M., and J. H. Isaacson, 1965 Genetic control over the inactivation of autosomal genes attached to the X-chromosome. Z. Vererbungsl. **96:** 313–323.

Cattanach, B. M., and P. Johnston, 1981 Evidence of non-random X-inactivation in the mouse. Hereditas **94:** 5.

Cattanach, B. M., and D. Papworth, 1981 Controlling elements in the mouse V. Linkage tests with X-linked genes. Genet. Res. **38:** 57–70.

Cattanach, B. M., and C. Rasberry, 1991 Identification of the *Mus spretus Xce* allele. Mouse Genome **89:** 565.

Cattanach, B. M., and C. Rasberry, 1994 Identification of the *Mus castaneus Xce* allele. Mouse Genome **92:** 114.

Cattanach, B. M., and C. E. Williams, 1972 Evidence of non-random X chromosome activity in the mouse. Genet. Res. **19:** 229–240.

Cattanach, B. M., C. E. Pollard and J. N. Perez, 1969 Controlling elements in the mouse X-chromosome. I. Interaction with the X-linked genes. Genet. Res. **14:** 223–235.

Chadwick, B. P., and H. F. Willard, 2001 Histone H2A variants and the inactive X chromosome: identification of a second macroH2A variant. Hum. Mol. Genet. **10:** 1101–1113.

Chao, W., K. D. Huynh, R. J. Spencer, L. S. Davidow and J. T. Lee, 2002 CTCF, a candidate trans-acting factor for X-inactivation choice. Science **295:** 345–347.

Costanzi, C., and J. R. Pehrson, 1998 Histone macroH2A1 is concentrated in the inactive X chromosome of female mammals. Nature **393:** 599–601.

Csankovszki, G., A. Nagy and R. Jaenisch, 2001 Synergism of Xist RNA, DNA methylation and histone hypoacetylation in maintaining X chromosome inactivation. J. Cell Biol. **153:** 773–783.

Favor, J., 1988 The mutagenic activity of ethylnitrosourea at low doses in spermatogonia of the mouse as assessed by the specific-locus test. Mutat. Res. **405:** 221–226.

Ferguson-Smith, A. C., and M. A. Surani, 2001 Imprinting and the epigenetic asymmetry between parental genomes. Science **293:** 1086–1089.

Habre de Angelis, M. H. F., H. Fuchs, B. Rathkolb, D. Soewarto, S. Marschall *et al.*, 2000 Genome-wide, large-scale production of mutant mice by ENU mutagenesis. Nat. Genet. **25:** 444–447.

Hatada, I., and T. Mukai, 1995 Genomic imprinting of p57/KIP2, a cyclin-dependent kinase inhibitor, in mouse. Nat. Genet. **11:** 204–206.

Heard, E., C. Rougeulle, D. Arnaud, P. Avner, C. D. Allis *et al.*, 2002 Methylation of histone H3 at Lys-9 is an early mark on the X chromosome during X inactivation. Cell **107:** 727–738.

Hentges, K., K. Thompson and A. Peterson, 1999 The *flat-top* gene is required for the expansion and regionalization of the telencephalic primordium. Development **126:** 1601–1609.

Hogan, B., R. Beddington, F. Costantini and E. Lacy, 1994 *Manipulating the Mouse Embryo.* Cold Spring Harbor Laboratory Press, Cold Spring Harbor, NY.

Howell, C. Y., T. H. Bestor, F. Ding, K. E. Latham, C. Mertineit *et al.*, 2001 Genomic imprinting disrupted by a maternal effect mutation in the Dnmt1 gene. Cell **104:** 829–838.

Huynh, K. D., and J. T. Lee, 2001 Imprinted X inactivation in eutherians: a model of gametic execution and zygotic relaxation. Curr. Opin. Cell Biol. **13:** 690–697.

Johnston, P. G., and B. M. Cattanach, 1981 Controlling elements in the mouse. IV. Evidence of non-random X-inactivation. Genet. Res. **37:** 151–160.

Jong, M. T., A. H. Carey, K. A. Caldwell, M. H. Lau, M. A. Handel *et al.*, 1999 Imprinting of a RING zinc-finger encoding gene in the mouse chromosome region homologous to the Prader-Willi syndrome genetic region. Hum. Mol. Genet. **8:** 795–803.

Justice, M. J., J. K. Noveroske, J. S. Weber, B. Zheng and A. Bradley, 1999 Mouse ENU mutagenesis. Hum. Mol. Genet. **8:** 1955–1963.

Kasarskis, A., K. Manova and K. V. Anderson, 1998 A phenotype-based screen for embryonic lethal mutations in the mouse. Proc. Natl. Acad. Sci. USA **95:** 7485–7490.

Lee, J. T., 2000 Disruption of imprinted X inactivation by parent-of-origin effects at *Tsix.* Cell **103:** 17–27.

Lee, J. T., and N. Lu, 1999 Targeted mutagenesis of Tsix leads to nonrandom X inactivation. Cell **99:** 47–57.

Lee, J. T., L. S. Davidow and D. Warshawsky, 1999 Tsix, a gene antisense to Xist at the X-inactivation centre. Nat. Genet. **21:** 400–404.

Leff, S. E., C. I. Brannan, M. L. Reed, T. Ozcelik, U. Francke *et al.*, 1992 Maternal imprinting of the mouse *Snrpn* gene and conserved linkage homology with the human Prader-Willi syndrome region. Nat. Genet. **2:** 259–264.

Lyon, M. F., 1961 Gene action in the X-chromosome of the mouse (*Mus musculus* L.). Nature **190:** 372–373.

Lyon, M. F., 1971 Possible mechanisms of X chromosome inactivation. Nature New Biol. **232:** 229–232.

Marin, I., M. L. Siegal and B. S. Baker, 2000 The evolution of dosage-compensation mechanisms. Bioessays **22:** 1106–1114.

Mise, N., Y. Goto, N. Nakajima and N. Takagi, 1999 Molecular cloning of antisense transcripts of the mouse *Xist* gene. Biochem. Biophys. Res. Commun. **258:** 537–541.

Nadeau, J. H., 2000 Muta-genetics or muta-genomics: the feasibility of large-scale mutagenesis and phenotyping programs. Mamm. Genome **11:** 603–607.

Nesbitt, M. N., 1971 X chromosome inactivation mosaicism in the mouse. Dev. Biol. **26:** 252–263.

Nolan, P., D. Kapfhamer and M. Bucan, 1997 Random mutagene-

sis screen for dominant behavioral mutations in mice. Methods **13:** 379–395.

Nolan, P. M., J. Peters, M. Strivens, D. Rogers, J. Hagan *et al.*, 2000 A systematic, genome-wide, phenotype-driven mutagenesis programme for gene function studies in the mouse. Nat. Genet. **25:** 440–443.

Pannuti, A., and J. C. Luchessi, 2000 Recycling to remodel: evolution of dosage-compensation complexes. Curr. Opin. Genet. Dev. **10:** 644–650.

Penny, G. D., G. F. Kay, S. A. Sheardown, S. Rastan and N. Brockdorff, 1996 The *Xist* gene is required in cis for X chromosome inactivation. Nature **379:** 131–137.

Percec, I., and M. S. Bartolomei, 2002 Do X chromosomes set boundaries? Science **295:** 287–288.

Percec, I., R. M. Plenge, J. H. Nadeau, M. S. Bartolomei and H. F. Willard, 2002 Autosomal dominant mutations affecting X inactivation choice in the mouse. Science **296:** 1136–1139.

Plenge, R. M., I. Percec, J. H. Nadeau and H. F. Willard, 2000 Expression-based assay of an X-linked gene to examine effects of the X-controlling element (*Xce*) locus. Mamm. Genome **11:** 405–408.

Prissette, M., O. El-Maarri, D. Arnaud, J. Walter and P. Avner, 2001 Methylation profiles of *DXPas34* during the onset of X-inactivation. Hum. Mol. Genet. **10:** 31–38.

Rastan, S., 1982 Primary non-random X-inactivation caused by controlling elements in the mouse demonstrated at the cellular level. Genet. Res. **40:** 139–147.

Rastan, S., 1983 Non-random X-chromosome inactivation in mouse X-autosome translocation embryos: location of the inactivation centre. J. Embryol. Exp. Morphol. **78:** 1–22.

Rastan, S., and B. M. Cattanach, 1983 Interaction between the Xce locus and imprinting of the paternal X chromosome in mouse yolk-sac endoderm. Nature **303:** 635–637.

Reik, W., W. Dean and J. Walter, 2001 Genomic imprinting: parental influence on the genome. Science **293:** 1089–1093.

Rugh, R., 1994 *The Mouse: Its Reproduction and Development.* Oxford University Press, Oxford.

Russell, L. B., 1963 Mammalian X-chromosome action: inactivation limited in spread and in region of origin. Science **140:** 976–978.

Russell, L. B., and N. L. Cacheiro, 1978 The use of mouse X-autosome translocations in the study of X-inactivation pathways and nonrandomness. Basic Life Sci. **12:** 393–416.

Russell, W. L., P. R. Hunsicker, D. A. Carpenter, C. V. Cornett and G. M. Guinn, 1982 Effect of dose-fractionation on the ethylnitrosurea induction of specific-locus mutations in mouse spermatogonia. Proc. Natl. Acad. Sci. USA **79:** 3592–3593.

Simmler, M. C., B. M. Cattanach, C. Rasberry, C. Rougeulle and P. Avner, 1993 Mapping the murine Xce locus with (CA)n repeats. Mamm. Genome **4:** 523–530.

Szabo, P. E., and J. R. Mann, 1995 Biallelic expression of imprinted genes in the mouse germ line: implications for erasure, establishment, and mechanisms of genomic imprinting. Genes Dev. **9:** 1857–1868.

Takagi, N., and M. Sasaki, 1975 Preferential inactivation of the paternally derived X chromosome in the extraembryonic membranes of the mouse. Nature **256:** 640–642.

Thorvaldsen, J. L., M. R. Mann, O. Nwoko, K. L. Duran and M. S. Bartolomei, 2002 Analysis of sequence upstream of the endogenous *H19* gene reveals elements both essential and dispensable for imprinting. Mol. Cell. Biol. **22:** 2450–2462.

Tsai, T.-F., K.-S. Chen, J. S. Weber, M. J. Justice and A. L. Beaudet, 2001 Evidence for translational regulation of the imprinted Snurf-Snrpn locus in mice. Hum. Mol. Genet. **11:** 1659–1668.

Weber, J. S., A. Salinger and M. J. Justice, 2000 Optimal N-ethyl-N-nitrosourea (ENU) doses for inbred mouse strains. Genesis **26:** 230–233.

West, J. D., and V. M. Chapman, 1978 Variation for X chromosome expression in mice detected by electrophoresis of phosphoglycerate kinase. Genet. Res. **32:** 91–102.

Wutz, A., and R. Jaenisch, 2000 A shift from reversible to irreversible X inactivation is triggered during ES cell differentiation. Mol. Cell **5:** 695–705.

Communicating editor: N. A. Jenkins